J. exp. Biol. **113**, 187–202 (1984)
Printed in Great Britain © *The Company of Biologists Limited 1984*

PULMONARY MECHANICS AND THE WORK OF BREATHING IN THE LIZARD, *GEKKO GECKO*

BY WILLIAM K. MILSOM AND TIMOTHY Z. VITALIS*

Department of Zoology, University of British Columbia, Vancouver, British Columbia, V6T 2A9, Canada

Accepted 9 April 1984

SUMMARY

Measurements of pulmonary mechanics made on anaesthetized specimens of the Tokay gecko *Gekko gecko* (Linné), indicate that both static and dynamic pulmonary mechanics are dominated by the mechanics of the body cavity and chest wall. The lungs are relatively large and compliant and offer little resistance to air flow at any of the ventilation frequencies (f) used in this study. The body wall is relatively stiff and becomes less compliant with increasing ventilation frequency and with increasing tidal volume (V_T) at the higher frequencies. The vast majority of the work performed in breathing is used to overcome elastic forces in the chest wall resisting lung inflation. This work increases exponentially with increases in volume. As a consequence, in terms of total ventilation, the most economic breathing pattern is a high frequency, low tidal volume pattern in which changes in minute ventilation ($\dot{V}_E$) are most economically produced solely by changes in f. Because reductions in tidal volume drastically reduce alveolar ventilation volume while dead space remains constant, the same arguments do not apply to alveolar minute ventilation ($\dot{V}_A$). In terms of alveolar minute ventilation, there is an optimum combination of f and V_T for each level of $\dot{V}_A$, with changes in $\dot{V}_A$ being most economically produced by almost equal changes in both f and V_T.

INTRODUCTION

In mammals, for each level of alveolar ventilation ($\dot{V}_A$), there is an optimum combination of tidal volume (V_T) and breathing frequency (f) which minimizes either the mechanical work of breathing (Otis, Fenn & Rahn, 1950) or the average force required from the respiratory muscles to move the lungs (Mead, 1960). It is energetically more expensive to ventilate the lungs at frequencies above or below these 'optimum' rates when corresponding adjustments are made in V_T to maintain $\dot{V}_A$ constant. Many studies have now shown that spontaneous breathing patterns in most mammals correspond closely with their calculated 'optimal' patterns (Christie, 1953; Agostoni, Thimm & Fenn, 1959; Crosfill & Widdicombe, 1961) particularly under conditions of elevated respiratory drive (Yamashiro, Daubenspeck, Lauritsen & Grodins, 1975).

* Present Address: School of Biological Sciences, University of East Anglia, Norwich, NR4 7TG, United Kingdom.

Key words: Reptiles, pulmonary mechanics, work of breathing.

Unlike the continuous breathing pattern of mammals, most reptiles exhibit a periodic or intermittent pattern of breathing in which single breaths or bursts of breaths are separated by breath-holds of varying length (McCutcheon, 1943; Gans & Hughes, 1967; Naifeh *et al.* 1970; Gans & Clark, 1976; Glass & Johansen, 1976). The primary regulated variable in respiratory responses to temperature change, hypoxia and hypercapnia, in most species, is the breath-hold length or non-ventilatory period (TNVP) (Glass & Johansen, 1976; Milsom & Jones, 1980; Benchetrit & Dejours, 1980). It is difficult to say to what extent these resting breathing patterns and ventilatory responses reflect the influence of mechanical factors as so little is known of pulmonary mechanics in this group. Static compliances of both isolated lungs and intact respiratory systems have been reported for a few species (Jackson, 1971; Cragg, 1978; Gratz, 1978; Hughes & Vergara, 1978; Perry & Duncker, 1978, 1980), and these data indicate that species with relatively stiff lungs (low compliance) tend to utilize a higher frequency and lower tidal volume breathing pattern than species with relatively high lung compliances. This implies that the resting breathing pattern may be strongly influenced by static lung mechanics (Perry & Duncker, 1980). Dynamic pulmonary mechanics, which would also be expected strongly to influence not only the resting breathing pattern but particularly the changes in breathing resulting from changes in respiratory drive, have not yet been described for any reptile. Since this information is essential for a full understanding of the interrelationship between pulmonary mechanics and breathing patterns in this group, the present study was undertaken to provide such data for one species of lizard, the Tokay gecko.

METHODS

Experiments were performed at room temperature (22–23 °C) on nine Tokay geckos (*Gekko gecko*) (36–151 g) anaesthetized by intraperitoneal injection of 25–30 mg kg^{-1} sodium pentobarbital (Somnotol, MTC Pharmaceuticals).

Static pressure-volume measurements

In all nine animals, an intratracheal cannula possessing a sidearm for pressure measurements was inserted into the trachea, just below the larynx, through a mid-ventral incision which was then sewn closed.

Resting lung volume (VLR) was determined by removing air from the lungs with a syringe, *via* the tracheal cannula, after opening the tracheal cannula to the atmosphere with the animals placed in a normal supine position. The lungs were then inflated to 10 cmH_2O pressure and allowed to return spontaneously to 0 cmH_2O pressure by opening the system to the atmosphere. The steady state pressure changes associated with a stepwise inflation, deflation and reinflation sequence of the lungs, were then recorded. Intratracheal pressure was measured with a Statham P23V pressure transducer and Gould d.c. amplifier and recorded on a Gould chart recorder.

In three animals, a mid-ventral incision was then made just anterior to the vent and a wide bore tube (5 mm i.d.) containing a sidearm for pressure measurements was inserted into the thoraco-abdominal cavity, sewn in place and the incision sealed. In this series of experiments, the intra-abdominal cavity pressure was monitored while the thoraco-abdominal cavity was inflated, deflated and reinflated in a stepwi

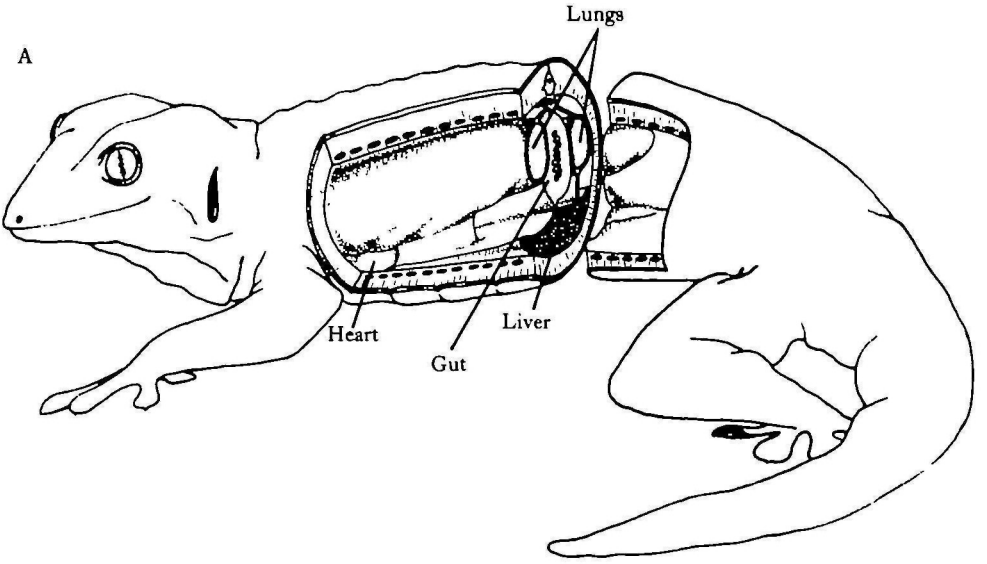

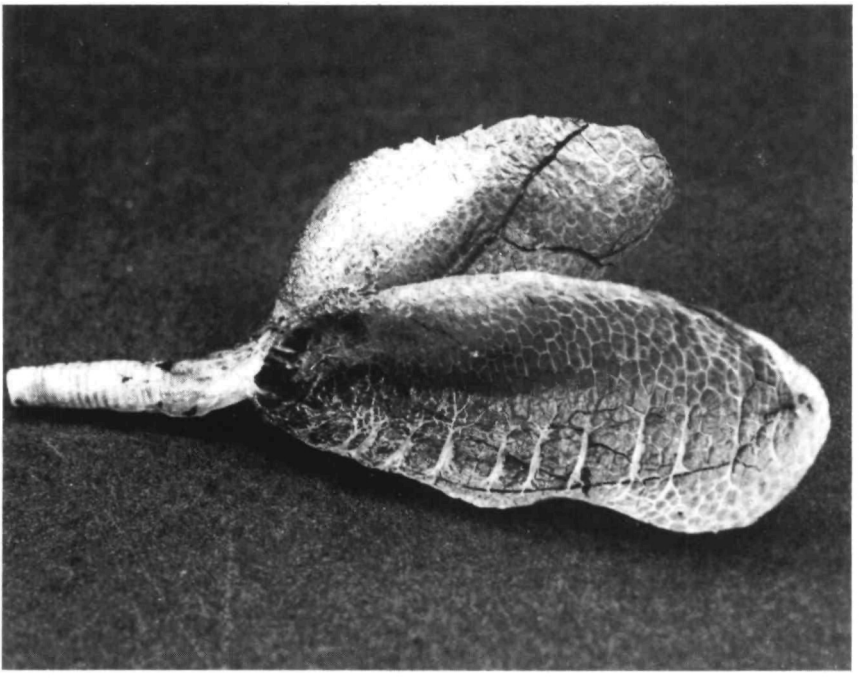

Fig. 1. (A) Schematic diagram of a Tokay gecko to show the location of the lungs in the body cavity and their relationship to the viscera and the body wall. (B) Dry cast of the lungs cut in longitudinal section to show internal structure; magnification, ×1·62.

fashion, beginning with the chest cavity equilibrated to atmospheric pressure and the animal, again, in the normal supine position.

In these three animals the body wall was then widely resected and the animals eviscerated. Then, starting from VLR the steady state pressure changes associated with a stepwise inflation, deflation and reinflation sequence of the exposed lungs, were recorded. The exposed lungs were periodically swabbed with saline throughout this procedure to prevent drying.

Dynamic pressure-volume measurements

In five of the remaining lizards, following the static pressure-volume measurements of the intact system, the tracheal cannula was connected to a pneumotachograph (Fleisch no. 00) which was in turn connected to a Harvard small animal respirator (Harvard Inc., Millis, Mass., U.S.A.). The pressure drop across the pneumotachograph screen during tracheal air flow was monitored with a Validyn DP 103-18 differential pressure transducer and this air flow signal was fed through a Gould integrating amplifier to give tidal volume. Intratracheal pressure was recorded as described for the static pressure-volume measurements. All measurements of pressure, flow and volume were continuously recorded on a Gould 6 channel chart recorder and the pressure and volume signals were also plotted on an Esterline Angus XY plotter. During pump ventilation, for any given lung volume, intratracheal pressure was always greater during inflation than during deflation. When volume was plotted against pressure on x,y coordinates, through a complete pump cycle, a counterclockwise rotating hysteresis loop was produced (Fig. 3A). Inflation volumes of 0·5–4 ml and ventilation frequencies of 3–120 min^{-1} were used in random sequence, to produce a spectrum of such dynamic pressure-volume loops.

In three lizards, a mid-ventral incision was then made just anterior to the vent and a large bore tube (5 mm i.d.) was inserted into the thoraco-abdominal cavity, as described earlier. This tube was then connected to the pneumotachograph and respirator and air flow and inflation volume were again recorded, along with abdominal cavity pressure (recorded as described above) during pump ventilation of the thoraco-abdominal cavity at frequencies between 3 and 120 min^{-1} with a tidal volume of 2 ml. Pressure and volume were again plotted on x,y coordinates to produce pressure-volume loops of each ventilation cycle. The lungs were collapsed during this procedure.

All values given in this paper are means ± S.E.

RESULTS

Anatomical observations

The lungs of the Tokay gecko are single chambered (unicameral), fused anteriorly, and share a common 'bronchial opening' arising from an undivided trachea (Fig. 1). Consequently, they lack an intrapulmonary bronchus, and internal partitioning is restricted to a series of dorsolateral ridges and a net-like system of tabeculae arising from the lung wall (faveoli). This faviform parenchyma is thickest (~2 mm) immediately caudal to the bronchial opening and reduced in the caudal regions where flattened trabeculae lie appressed to the lung wall (Fig. 1, Perry & Duncker, 1978).

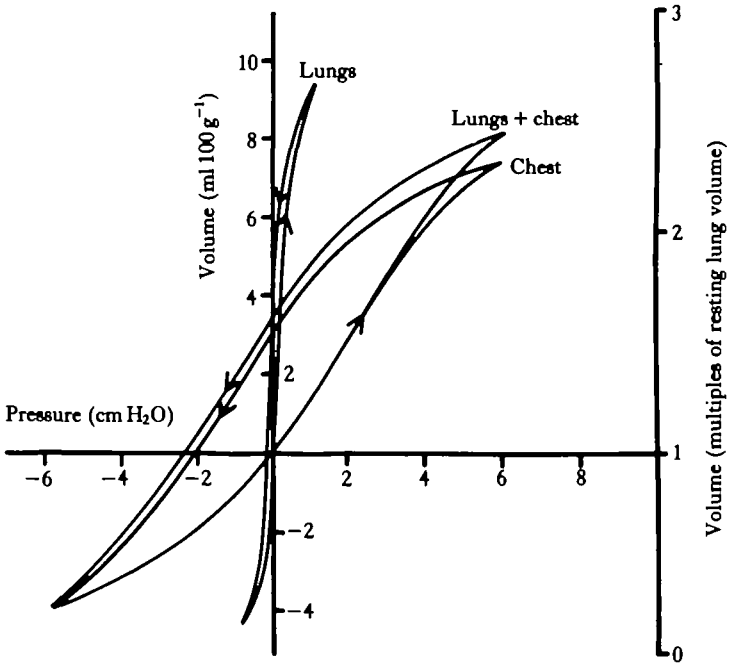

Fig. 2. Static pressure-volume diagrams from one animal for the lungs, chest wall and lung and chest wall together. Volume is expressed both in absolute values (left axis) (zero volume is defined in the text) and as multiples of the resting lung volume. Arrows indicate the path of inflation and deflation.

The lungs are not enclosed in a pleural cavity but lie along the dorsal surface of the pleuroperitoneal cavity, held in place by thin mesopneumonia. A dorsal mesopneumonium connects the dorsomedial surface of each lung to the dorsal body wall while a smaller ventral mesopneumonium anchors the ventromedial lung surface to the liver and underlying viscera (Fig. 1). These connections do not hinder the free movement of the lungs but do establish the resting lung volume when the system is open to the atmosphere.

Static pressure-volume measurements

Fig. 2 depicts sample static pressure-volume curves derived from one animal. Static compliance of the body wall (C_B), lungs (C_L) and intact system (total compliance, C_T) were taken as the mid-range slope of the pressure-volume curves obtained during step inflation of the body cavity, lungs and intact system respectively. Based on data collected from all animals, V_{LR} was $6{\cdot}3 \pm 1{\cdot}0$ ml $100\,g^{-1}$ ($N = 9$) and the average values for C_L, C_B and C_T were $20{\cdot}0 \pm 3{\cdot}0$ ($N = 3$), $1{\cdot}45 \pm 0{\cdot}5$ ($N = 3$) and $1{\cdot}55 \pm 0{\cdot}4$ ml cmH_2O^{-1} $100\,g^{-1}$ respectively. Because of the high compliance of the lung, the compliance of the total system closely reflects the compliance of the body wall.

Dynamic pressure-volume measurements

Fig. 3A shows a schematic diagram of a single, representative, dynamic pressure-volume loop to illustrate the procedure used for determining the dynamic compliance

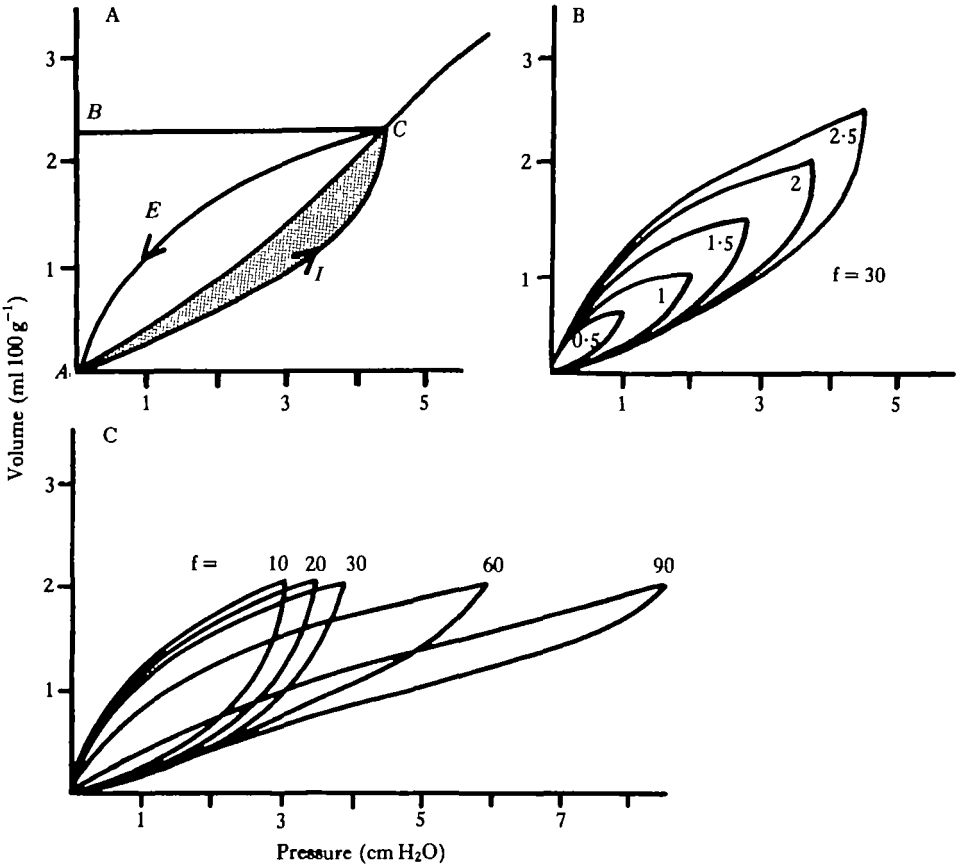

Fig. 3. (A) Schematic diagram of the pressure-volume relations of the intact respiratory system during a ventilation cycle. The loop begins at *A* and is generated by a point, moving with time, in a counter-clockwise direction. See text for details. (B) Effects of increasing tidal volume from 0·5 to 2·5 ml $100\,g^{-1}$ on pressure-volume loops produced at a constant ventilation frequency of $30\,min^{-1}$ in one individual. (C) Effects of increasing ventilation frequency from 10 to $90\,min^{-1}$ on pressure-volume loops produced for a constant tidal volume of 2 ml $100\,g^{-1}$ in the same individual as in (B).

and the work of ventilation. Dynamic compliance was taken as the slope of the line connecting points of zero flow (end-inflation and end-deflation) on the pressure-volume loops obtained during pump ventilation. For any given pump inflation, the area subtended between the compliance curve for the intact system and the volume axis of a pressure-volume diagram (area *ABCA* in Fig. 3A) was taken to represent the work which was performed to overcome elastic forces opposing that inflation (Otis, 1964). During this inflation, however, work was also performed to overcome flow-resistive forces, the magnitude of which depended on the flow resistance and rate of movement of gas and tissues. In Fig. 3A, the horizontal distance between the dynamic compliance curve, *AC*, and the curved portion of the pressure volume loop, *AIC*, represents the pressure gradient required to overcome these non-elastic forces during that lung inflation. The area bounded by these two curves, area *AICA*, was the work required to overcome the non-elastic forces (Otis, 1964). Together, these two components of work sum to equal the total work of inflation. In these pump-ventilated

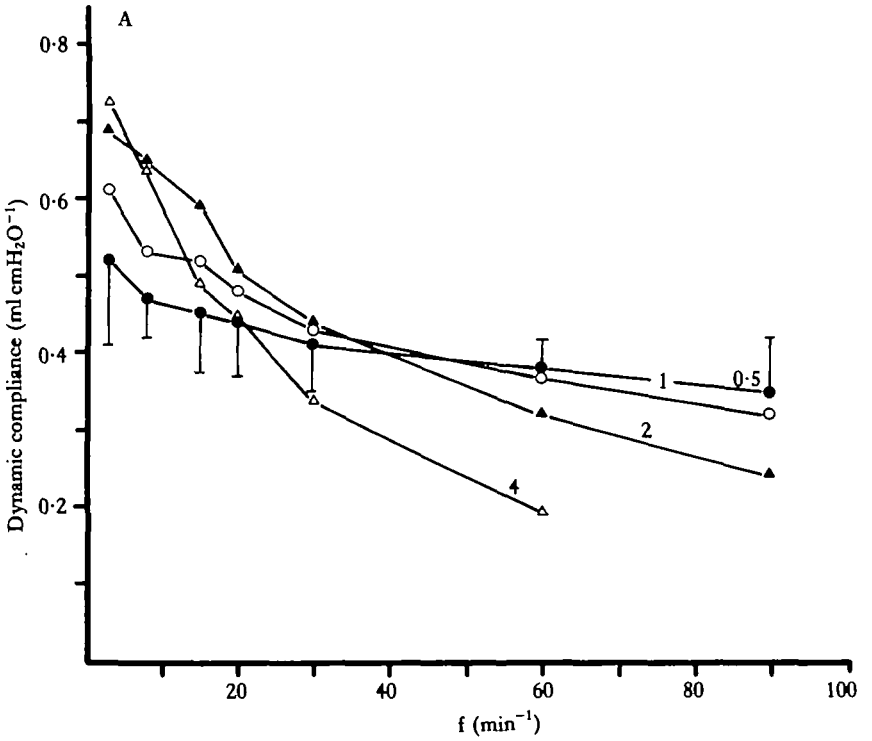
A
0·8
0·6
0·4
0·2
Dynamic compliance (ml cmH2O-1)
1
0·5
2
4
20
40
60
80
100
f (min-1)

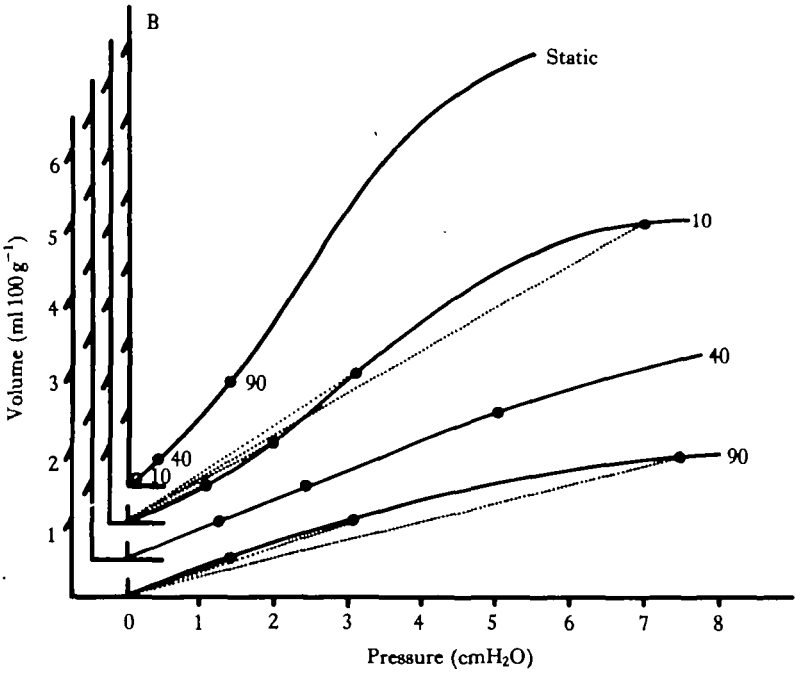
B
Static
10
40
90
90
40
10
6
5
4
3
2
1
Volume (ml 100 g-1)
0
1
2
3
4
5
6
7
8
Pressure (cmH2O)

Fig. 4

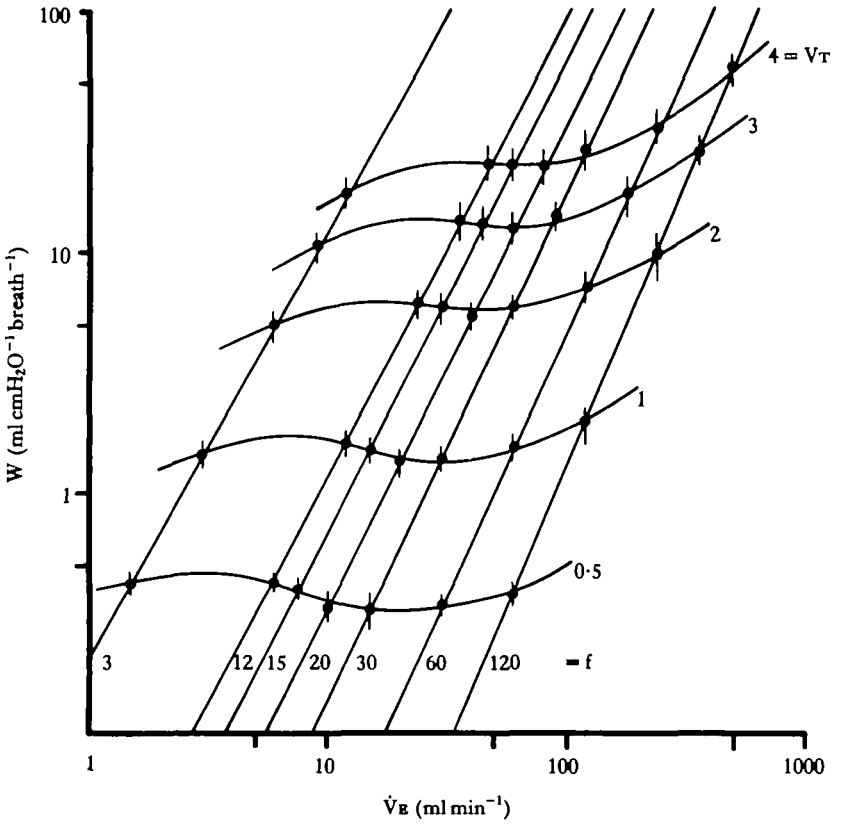

Fig. 5. The relationship between the total work breath^{-1} (W) and minute ventilation ($\dot{V}_E$) for different combinations of tidal volume (V_T in ml) and respiratory frequency (f in breaths min^{-1}). Data points represent average values from five animals and vertical bars represent ±1 S.E.M.

animals, deflation is a passive event, the pressure and volume falling along the line *CEA* in Fig. 3A and being powered by the elastic energy stored during lung inflation. Thus the total work of an entire ventilation cycle is equal to the work required to overcome elastic and non-elastic forces during inflation. The magnitude of each of these components of work was determined by measuring the respective areas represented graphically by planimeter. Minute work is simply the product of the total work per breath multiplied by the number of breaths per minute.

Fig. 3B shows data collected from a single animal illustrating the effects of increasing inflation volume at a constant ventilation frequency on dynamic pressure-volume loops and in Fig. 3C, the effects of increasing ventilation frequency at a constant tidal volume are shown for the same animal. The changes in slope of the hysteresis loops, so evident in Fig. 3C, are indicative of changes in the dynamic compliance of the respiratory system. The changes in dynamic compliance recorded over the entire range of tidal volumes (V_T) and breathing frequencies (f) used in these studies,

Fig. 4. (A) The relationship between ventilation frequency and the dynamic compliance of the intact respiratory system. Each curve was derived for a single tidal volume (0·5 to 4 ml) from average values for five animals. Standard error bars are omitted from all but one curve, for clarity, but are quantitatively similar for each curve. (B) The relationship between peak inspiratory pressure and tidal volume for lung inflations at 10, 40 and 90 breaths min^{-1}. The slopes of the dotted lines represent dynamic compliances. The static pressure-volume curve is included for comparison and to demonstrate the true origins (open circles) of each of the frequency curves.

derived from the mean values taken from all five animals, are shown in Fig. 4A Standard error bars have been included for only one tidal volume curve in this figure, for clarity, but were quantitatively similar for each curve. At the lowest ventilation frequencies ($<10\,min^{-1}$), increases in tidal volume lead to an increase in dynamic compliance (a decrease in stiffness), whereas at high ventilation frequencies ($>60\,min^{-1}$) increases in tidal volume lead to a decrease in dynamic compliance (increase in stiffness). For tidal volumes between 0·5 and 2 ml, dynamic compliance is relatively volume-independent over a frequency range from 30–50 min^{-1} (Figs 3B, 4A). For any given tidal volume, increasing frequency leads to a decrease in dynamic compliance, an effect which is accentuated with increasing tidal volume. In the series of curves in Fig. 4B, the peak pressures associated with lung inflation of various tidal volumes at 10, 40 and 90 breaths min^{-1} are plotted along with the static pressure-volume curve for comparison. In these curves, the slopes (dotted lines) connecting the data points to the origin of each curve, represent dynamic compliance. The origins of each of the frequency curves have been artificially set to zero pressure and volume. As ventilation frequency increases, the time available for passive expiration decreases. As a consequence, each time ventilation frequency is increased, there is a transient

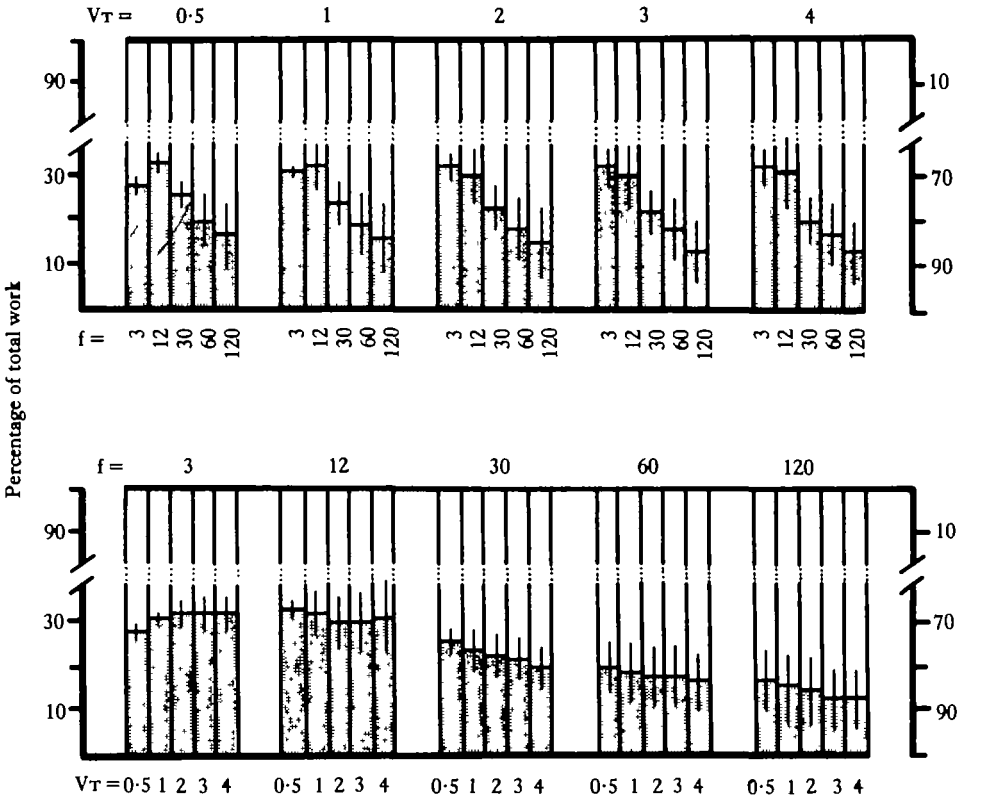

Fig. 6. The percentage of total work required to overcome non-elastic forces (stippled bars, left hand axis, read from bottom to top) and elastic forces (clear bars, right hand axis, read from top to bottom). In the upper panel, the effects of increasing ventilation frequency (f) from 3 to 120 min^{-1} are shown for different tidal volumes (V_T) from 0·5 to 4 ml. In the lower panel, the effects of increasing tidal volume from 0·5 to 4 ml are shown for different ventilation frequencies from 3 to 120 min^{-1}.

phase during which expiration is less than the previous inflation, leading to a small increase in end-expiratory lung volume (functional residual capacity, FRC). This increase in FRC also increases the elastic recoil of the lung which promotes an increase in expiratory air flow returning the system to equilibrium (expiration = inspiration). The actual starting values for each curve are depicted by open circles on the static pressure-volume curve. All three points fall on the relatively linear portion of this curve. As a consequence, the decreases in dynamic compliance associated with increasing frequency cannot have been caused by shifting the starting point of each ventilation to a volume at which the system as a whole is stiffer, but – as seen by the shape of each curve – must be the result of a genuine increase in dynamic compliance.

In the three animals for which the body cavity alone was ventilated at increasing frequencies, but only for a single tidal volume, similar changes in dynamic compliance were observed. These results would suggest that the changes in dynamic compliance recorded here represent changes in the mechanics of the body wall.

Increasing tidal volume at any given ventilation frequency, produces a straight line on the log.log plot shown in Fig. 5, indicating that there is an exponential increase in the work breath^{-1}. The curves produced by increasing ventilation frequency at each tidal volume, are more complex. Each curve shows an initial range, at low frequencies ($<10\,min^{-1}$) in which the work breath^{-1} increases with increasing frequency. This is followed by a range in which the work breath^{-1} stabilizes or actually decreases as

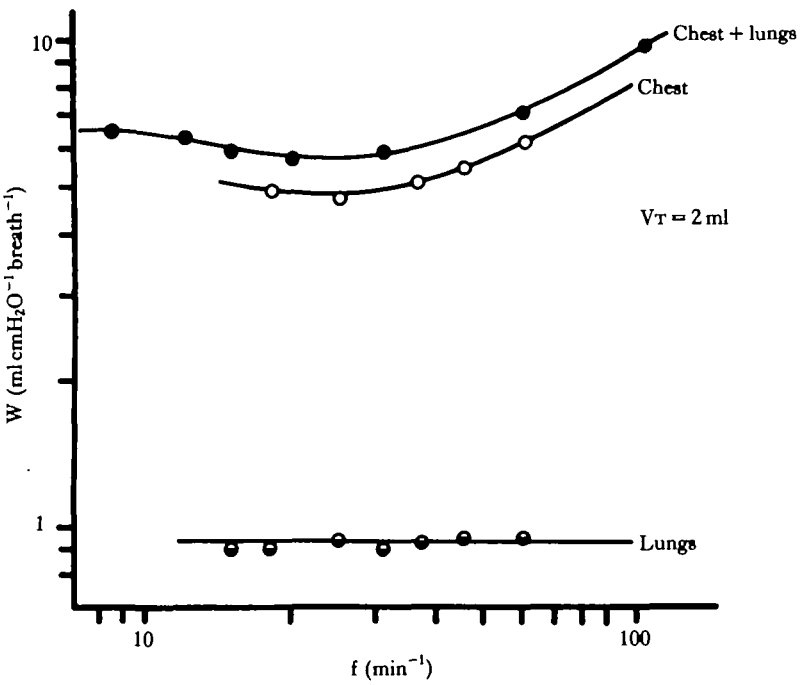

Fig. 7. The relationship between the work breath^{-1} (W) and ventilation frequency (f) for the intact respiratory system (chest and lungs), the body wall alone (chest) and the lungs alone (lungs). Data are for one animal and values used to describe the lung curve were derived by subtracting the chest curve from the chest and lung curve. Tidal volume was 2 ml.

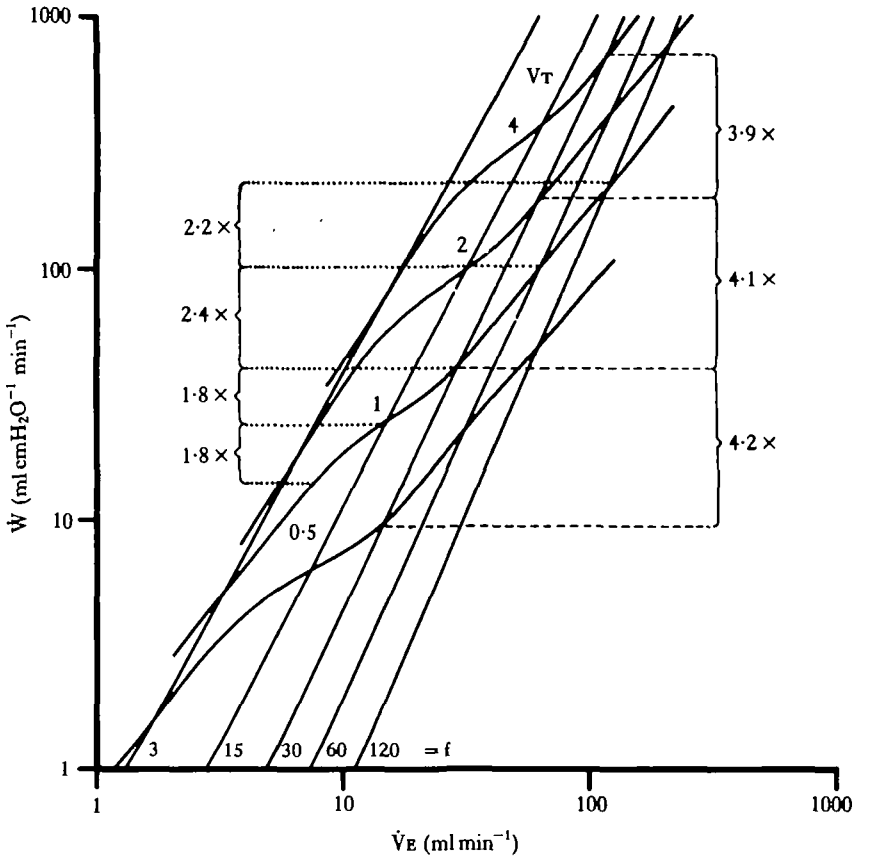

Fig. 8. The relationship between minute work ($\dot{W}$) and minute ventilation ($\dot{V}_E$) for different combinations of ventilation volume (V_T in ml) and frequency (f min^{-1}). The effects on minute work of doubling $\dot{V}_E$ by increasing f at a constant V_T of 1 ml are shown by the numbers and dotted lines on the left side of the figure while the effects of doubling $\dot{V}_E$ on minute work by increasing V_T at a constant f of 30 min^{-1} are shown by the numbers and dashed lines on the right side of the figure.

frequency increases, and this in turn gives rise to a third range in which the work $breath^{-1}$ again increases with further increases in ventilation frequency (>60 min^{-1}). The overall slope of each tidal volume curve increases with tidal volume.

Non-elastic work plays a much smaller role in the generation of total work, than does elastic work (Fig. 6). The contribution of non-elastic work to total work decreases slightly as tidal volume increases at ventilation frequencies above 12 min^{-1} but, in general, decreases substantially as ventilation frequency increases (above 12 min^{-1}) for any given tidal volume.

Data obtained from the dynamic pressure-volume loops of the isolated chest (Fig. 7) indicate that the relationships observed between the work $breath^{-1}$ and ventilation frequency and tidal volume, recorded in the intact animal, primarily reflect the dynamic properties of the chest wall rather than any inherent mechanical properties of the lung itself. The calculated cost of ventilating the lung alone is low and frequency-independent over the range studied here.

In Fig. 8, the data from Fig. 5 are replotted as minute work ($\dot{W}$), the product of

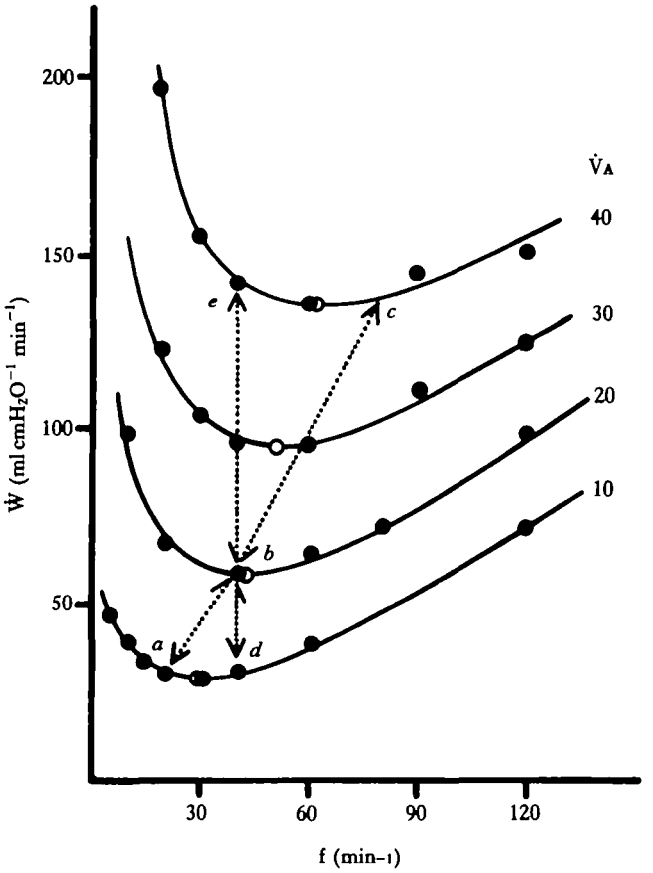

Fig. 9. Relationship between minute work ($\dot{W}$) and ventilation frequency (f) for several levels of alveolar minute ventilation ($\dot{V}_A$ in ml min^{-1} 100 g^{-1}). Closed circles represent data points derived from Fig. 5, as described in the text and the open circles denote the value of f for which each curve exhibits its minimum value of $\dot{W}$. Points *a*, *b* and *c* represent a V_T of 1 ml on each respective curve. Points *d*, *b* and *e* are points of equal ventilation frequency. The effects on $\dot{W}$ of increasing $\dot{V}_A$ by doubling V_T at constant f, or doubling f at constant V_T are represented by the vertical distance between points of equal f or equal V_T, respectively, on each $\dot{V}_A$ curve.

the work required to produce a single breath (W) and the number of breaths taken each minute (f). It can be seen from this figure, that the work required to produce any given level of minute ventilation ($\dot{V}_E$) is less the higher the ventilation frequency and the lower the tidal volume. Furthermore, increases in $\dot{V}_E$ are most economically effected by increasing breathing frequency, rather than increasing tidal volume. As illustrated in Fig. 8, a doubling of $\dot{V}_E$, brought about solely by doubling ventilation frequency, at a V_T of 1 ml, will increase minute work 1·8 to 2·4 times. If $\dot{V}_E$ is doubled, solely by increasing V_T, at a ventilation frequency of 30 min^{-1}, minute work increases by 3·9 to 4·2 times.

The effects of changing ventilation volume and frequency on minute work are examined for constant levels of alveolar minute ventilation ($\dot{V}_A$) in Fig. 9. $\dot{V}_A$ is the product of the alveolar ventilation volume [V_A = tidal volume (V_T) − dead space volume (V_D)] and ventilation frequency. The values used to construct this figure were calculated from the plots shown in Fig. 5 using the value for V_D of 0·50

($\pm 0{\cdot}03$) ml $100\,g^{-1}$, recorded for these animals (Milsom, 1984). It can be seen from this figure that for each level of $\dot{V}_A$, there is a single combination of f and V_T for which $\dot{W}$ is minimum. For any given level of $\dot{V}_A$, the relationship described here can be represented by the equation $\dot{W} = (60f/2C_L)(V_T)^2$.

In Fig. 9, the consequences of doubling $\dot{V}_A$ by increasing ventilation frequency alone or by increasing alveolar ventilation volume alone are also shown. Both methods of increasing alveolar minute ventilation lead to increases in minute work of 1·8 to 2·3 times. The least expensive way of increasing $\dot{V}_A$, i.e. the changes associated with the transition between the optimum patterns associated with each level of $\dot{V}_A$, involves roughly equal changes in both f and V_T.

DISCUSSION

Given the extremely simple structure of the lungs of the Tokay gecko (Fig. 1) (Perry & Duncker, 1978), all viscoelastic properties of the lung must reside in the outer lung wall. The static pressure-volume relationships reveal that these lungs are extremely compliant, so much so that the total compliance of the intact respiratory system is almost identical to the compliance of the body wall ($C_T \simeq C_B$) (Fig. 2). Our values of C_B and C_T are somewhat lower than those previously reported for this species (Perry & Duncker, 1978) but in general, are consistent with values reported for other species of lizards possessing unicameral lungs (Table 1). In mammals of similar size (Table 1), values reported for C_B are similar to those reported for lizards but the lungs are, in comparison, extremely stiff and consequently, C_T, the compliance of the total intact system, is much lower.

The dynamic compliance of the respiratory system of the gecko, is frequency-dependent. For any tidal volume, the higher the ventilation frequency, the stiffer the behaviour of the system, an effect which is enhanced by increasing tidal volume. This decrease in compliance (increasing stiffness) with increasing frequency appears to be due solely to viscoelastic properties of the body wall.

Interestingly, at low ventilation frequencies, dynamic compliance increases as tidal volume increases, while at high ventilation frequencies, dynamic compliance decreases as tidal volume increases. For tidal volumes between 0·5 and 2 ml, dynamic compliance is relatively volume-independent between 35 and 50 breaths min^{-1}. These changing relationships stem from the shift in the shape of the pressure-volume relationships from a sigmoid pressure-volume curve under static conditions and at low ventilation frequencies to a hyperbolic pressure-volume curve at high ventilation frequencies. At very low frequencies and under static conditions, there is a range in the inflation curve where the relative increase in pressure required to produce a given increase in volume is reduced. This may reflect the effects of geometric change. The law of Laplace would predict that the geometric changes accompanying increased body volume should result in a reduction in the apparent stiffness of the system. This geometric effect would ultimately be offset by decreased elasticity at large body volumes. At higher ventilation frequencies, this effect is absent and it requires progressively greater increases in pressure to produce equal increases in volume. Frequency-related increases in the dynamic compliance of the body wall material more than offset any advantage of geometric changes. As a consequence, the cost o

Table 1. *Mean lung volumes and compliances of various species*

Species	Weight (g)	V_{LR} (ml)	C_T $\left(\frac{ml}{cmH_2O}\right)$	C_T $\left(\frac{ml}{cmH_2O/ml V_{LR}}\right)$	C_L $\left(\frac{ml}{cmH_2O}\right)$	C_L $\left(\frac{ml}{cmH_2O/ml V_{LR}}\right)$	C_B $\left(\frac{ml}{cmH_2O}\right)$	C_B $\left(\frac{ml}{cmH_2O/ml V_{LR}}\right)$	Reference
Teju lizard	701 ± 330·5	30·7 ± 13·01	13·65 ± 4·23	0·44	—	—	—	—	Perry & Dunker, 1978
Green lizard	28 ± 4·4	1·3 ± 1·3	0·51 ± 0·18	0·39	1·74 ± 0·54	1·34	0·72*§	0·55§	Perry & Dunker, 1978
Tokay lizard (gecko)	108 ± 47	7·0 ± 1·1	5·08 ± 0·39	0·73	29·53 ± 13·37	4·22	6·14§	0·88§	Perry & Dunker, 1978
	100 ± 21	6·3 ± 1·0	1·55 ± 0·40	0·25	20·0 ± 3·0	3·17	1·45 ± 0·50	0·23	This study
Mouse	32	0·29	0·04†	0·09†	0·05	0·11	0·33	0·68	Crosfill & Widdicombe, 1961
Rat	250	1·55	0·31†	0·10†	0·39	0·12	1·47	0·55	Crosfill & Widdicombe, 1961

* Value listed for C_B in original paper is actually $1/C_B$.
† Calculated from C_L and C_B values using $1/C_T = 1/C_L + 1/C_B$.
§ Calculated from C_L and C_T values using $1/C_T = 1/C_L + 1/C_B$.

increasing tidal volume is much greater at high ventilation frequencies than at low frequencies. This is also evident in the work breath^{-1} curves (Fig. 5).

The work required to produce each breath is primarily expended in overcoming forces associated with movement of the body cavity and chest wall. Elastic forces account for most of this work. The work required to move the lung is relatively small (<15 % of total work) and frequency-independent, implying that non-elastic work associated with resistance to air flow is negligible in the gecko lung over the range of ventilation frequencies used in this study.

For any given ventilation frequency, the work required to produce each breath increases as an exponential function as tidal volume increases. This appears to be due to the material properties of the body cavity and chest wall, and this effect is slightly accentuated at higher breathing frequencies due to the decreased dynamic compliance. Elastic work accounts for roughly 70 to 85 % of the total work and this fractional contribution tends to increase slightly, although not significantly, as V_T increases at higher ventilation frequencies.

The relationship between the work per breath and breathing frequency for any given tidal volume is complex and indicative of a multicomponent system with more than one time constant. As ventilation frequency increases from 0 to 10 breaths min^{-1}, the work breath^{-1} also increases. Over the range of ventilation frequencies from 10 to 30 breaths min^{-1}, however, work breath^{-1} decreases slightly. At ventilation frequencies above 60 min^{-1}, work breath^{-1} again increases with increasing frequency. This latter increase is more pronounced at larger tidal volumes. Increases in the non-elastic work breath^{-1} with increasing frequency are not surprising, and would be expected to be larger at higher tidal volumes and ventilation frequencies. The decrease in work breath^{-1} over the mid range from 10 to 30 breaths min^{-1} is surprising particularly as it is almost exclusively due to a decrease in non-elastic work. Over this range of ventilation frequencies there is an apparent decrease in the viscoelasticity of the body cavity and chest wall. At present, we are unable to account for this effect.

The results of the work breath^{-1} measurements indicate that it is relatively expensive to increase tidal volume and that increases in ventilation frequency are a more economical way to increase $\dot{V}_E$. This is even more evident from the minute work curves. For any given $\dot{V}_E$, the higher the breathing frequency and lower the tidal volume, the less the cost of breathing. Increases in $\dot{V}_E$ brought about solely by increasing f are half the cost of similar increases in $\dot{V}_E$ brought about solely by increasing V_T. These results are consistent with theoretical predictions for a purely elastic system. This correlates well with the fact that the work required to overcome elastic forces accounts for 70–85 % of the total work in this system.

Tidal volume (V_T) is equal to alveolar ventilation volume (V_A) + dead space volume (V_D). V_D is anatomically fixed, and therefore, as V_T is reduced, V_A is reduced while V_D remains constant, and V_D becomes a proportionately greater fraction of V_T. Thus, for any given level of $\dot{V}_E$, as f increases with concomitant decreases in V_T, the percentage of the total work which goes into moving dead space gas increases. Despite further decreases in the work breath^{-1}, below the point where $V_T = V_D$ (i.e. $V_A = 0$), the lungs are no longer ventilated, revealing an extremely false economy (Otis, 1954). If minute work is expressed as a function of ventilation frequency for levels of constant alveolar minute ventilation, $\dot{V}_A$, the resulting curves reveal that, as for mammals, fo

each level of $\dot{V}_A$ there is an optimum combination of f and V_A (and hence V_T) where the work of breathing is minimum. It is of interest that for the levels of $\dot{V}_A$ calculated here, increases in f and V_T are equally efficient means of increasing $\dot{V}_A$.

In mammals, pulmonary mechanics are most strongly influenced by the mechanics of the lungs. Both elastic and non-elastic forces are important in generating the work required for breathing. The non-elastic forces required to overcome resistance to air flow predominate at higher ventilation frequencies. In lizards, both static and dynamic mechanics are most strongly influenced by the mechanics of the body cavity and chest wall. The vast majority of the work of breathing is required to overcome elastic forces alone, whatever the ventilation frequency. Despite these striking differences between the pulmonary mechanics of each group, in both groups there is an optimum combination of f and V_T at which minute work is at a minimum for each level of $\dot{V}_A$. These optima represent an interaction between pulmonary mechanics and the relative costs of dead space ventilation, and it would appear that such relationships hold for species with vast differences in pulmonary mechanics. The physiological significance of these results to the normal breathing pattern in the Tokay gecko will be considered in the following paper.

The authors wish to thank Dr Peter Pare for his advice and suggestions and Dr John Gosline for his patient and valuable assistance throughout the data analysis and writing of this paper. This study was supported by grants from the Natural Sciences and Engineering Council of Canada and the Natural, Applied and Health Sciences Committee of the University of British Columbia.

REFERENCES

AGOSTONI, E., THIMM, F. F. & FENN, W. O. (1959). Comparative features of the mechanics of breathing. *J. appl. Physiol.* **14**, 679–683.

BENCHETRIT, B. & DEJOURS, P. (1980). Ventilatory CO_2 drive in the tortoise *Testudo horsfeldi*. *J. exp. Biol.* **87**, 229–236.

CHRISTIE, R. V. (1953). Dyspnoea in relation to the visco-elastic properties of the lungs. *Proc. R. Soc. Med.* **46**, 381–386.

CRAGG, P. A. (1978). Ventilatory patterns and variables in rest and activity in the lizard, *Lacerta*. *Comp. Biochem. Physiol.* **60**A, 399–410.

CROSFILL, M. L. & WIDDICOMBE, J. G. (1961). Physical characteristics of the chest and lungs and the work of breathing in different mammalian species. *J. Physiol., Lond.* **158**, 1–14.

GANS, C. & CLARK, B. (1976). Studies on ventilation of *Caiman crocodilus* (Crocodilia: Reptilia). *Respir. Physiol.* **26**, 285–301.

GANS, C. & HUGHES, G. M. (1967). The mechanism of lung ventilation in the tortoise *Testudo graeca* Linne. *J. exp. Biol.* **47**, 1–20.

GLASS, M. & JOHANSEN, K. (1976). Control of breathing in *Acrochordus javanicus*, an aquatic snake. *Physiol. Zool.* **49**, 328–340.

GRATZ, R. K. (1978). Ventilation and gas exchange in the diamondback water snake, *Natrix rhombifera*. *J. comp. Physiol.* **127**, 299–305.

HUGHES, G. M. & VERGARA, G. A. (1978). Static pressure-volume curves for the lung of the frog (*Rana pipiens*). *J. exp. Biol.* **76**, 149–165.

JACKSON, D. C. (1971). Mechanical basis for lung volume variability in the turtle, *Pseudemys scripta elegans*. *Am. J. Physiol.* **220**, 754–758.

MCCUTCHEON, F. H. (1943). The respiratory mechanism in turtles. *Physiol. Zool.* **16**, 255–269.

MEAD, J. (1960). Control of respiratory frequency. *J. appl. Physiol.* **15**, 325–336.

MILSOM, W. K. (1984). The interrelationship between pulmonary mechanics and spontaneous breathing pattern in the Tokay lizard, *Gekko gecko*. *J. exp. Biol.* **113**, 203–214.

MILSOM, W. K. & JONES, D. R. (1980). The role of vagal afferent information and hypercapnia in control of the breathing pattern in Chelonia. *J. exp. Biol.* **87**, 53–63.

NAIFEH, K. H., HUGGINS, S. E., HOFF, H. E., HUGG, T. W. & NORTON, R. E. (1970). Respiratory patterns in crocodilian reptiles. *Respir. Physiol.* **9**, 31–42.

OTIS, A. B. (1954). The work of breathing. *Physiol. Rev.* **34**, 449–458.

OTIS, A. B. (1964). The work of breathing. In *Handbook of Physiology*, Section 3, Vol. 1, *Respiration*, (eds W. O. Fenn & H. Rahn). Washington D.C.: American Physiological Society.

OTIS, A. B., FENN, W. O. & RAHN, H. (1950). The mechanics of breathing in man. *J. appl. Physiol.* **2**, 592–607.

PERRY, S. F. & DUNCKER, H. R. (1978). Lung architecture, volume and static mechanics in five species of lizards. *Respir. Physiol.* **34**, 61–81.

PERRY, S. F. & DUNCKER, H. R. (1980). Interrelationship of static mechanical factors and anatomical structure in lung evolution. *J. comp. Physiol.* **138**, 321–334.

YAMASHIRO, S. M., DAUBENSPECK, J. A., LAURITSEN, T. N. & GRODINS, F. S. (1975). Total work rate of breathing optimization in CO_2 inhalation and exercise. *J. appl. Physiol.* **38**, 702–709.